Research Square

Preprints are preliminary reports that have not undergone peer review.
They should not be considered conclusive, used to inform clinical practice,
or referenced by the media as validated information.

Impact of Climate Warming on Oncomelania hupensis in China- Multi-scale Evidence

Qin Li
National Institute for Parasitic Diseases
Jin-Xin Zheng
Shanghai Jiao Tong University
Li-Juan Zhang
National Institute for Parasitic Diseases
Su-ying Guo
National Institute for Parasitic Diseases
Ying Yang
National Institute for Parasitic Diseases
Jüerg Utzinger
Swiss Tropical and Public Health Institute
Xiao-Nong Zhou
National Institute for Parasitic Diseases
Jing Xu
xujing@nipd.chinacdc.cn

National Institute for Parasitic Diseases
Shi-Zhu Li
National Institute for Parasitic Diseases

Research Article

Keywords: Oncomelania hupensis, Climate warming, Land use, Temperature, Time window

Posted Date: February 17th, 2026

DOI: https://doi.org/10.21203/rs.3.rs-8804450/v1

License: This work is licensed under a Creative Commons Attribution 4.0 International License.
Read Full License

Additional Declarations: No competing interests reported.

Version of Record: A version of this preprint was published at Infectious Diseases of Poverty on July 3rd, 2026. See the published version at https://doi.org/10.1186/s40249-026-01475-0.

Impact of Climate Warming on *Oncomelania hupensis in China*-Multi-scale Evidence

Qin Li[1], Jin-Xin Zheng[2], Li-Juan Zhang[1], Su-ying Guo[1], Ying Yang[1], Jüerg Utzinger[3], Xiao-Nong Zhou[1,2], Jing Xu[1,2*], Shi-Zhu Li[1*]

[1] National Key Laboratory of Intelligent Tracking and Forecasting for Infectious Diseases, National Institute of Parasitic Diseases at Chinese Center for Disease Control and Prevention (Chinese Center for Tropical Diseases Research), NHC Key Laboratory of Parasite and Vector Biology, WHO Collaborating Centre for Tropical Diseases, National Center for International Research on Tropical Diseases, Shanghai 200025, China.
[2] School of Global Health, Chinese Center for Tropical Diseases Research, Shanghai Jiao Tong University School of Medicine, Shanghai 200025, China.
[3] Swiss Tropical and Public Health Institute, Kreuzstrasse 2, CH–4123 Allschwil, Switzerland.

Qin Li: liqinchina@163.com
Jin-Xin Zheng: jamesjin63@163.com
Li-Juan Zhang: zhanglj@nipd.chinacdc.cn
Su-ying Guo: guosy@nipd.chinacdc.cn
Ying Yang: yangying@nipd.chinacdc.cn
Jürg Utzinger: Juerg.Utzinger@swisstph.ch
Xiao-Nong Zhou: zhouxn1@chinacdc.cn
* Corresponding author: Jing Xu: xujing@nipd.chinacdc.cn
Shi-Zhu Li: lisz@chinacdc.cn

Abstract:

Background: Climate warming is increasingly reshaping the population dynamics of *Oncomelania hupensis*, the sole intermediate host of *Schistosoma japonicum* in China. Investigating the response of *O. hupensis* to climate warming is crucial for guiding targeted and precise interventions against these snails, thereby accelerating progress towards schistosomiasis elimination in China.

Method: We conducted temperature-controlled laboratory experiments to quantify survival, body size, and body weight responses of individual *O. hupensis* under non-optimal temperatures. We then developed sliding-window models based on long-term (1990-2022) population surveys and climate data, examining climate exposure across its life stages to assess population-level responses to climate warming; and used general linear mixed-effect models to explore the environmental factors of climate responses (geographic: latitude, longitude, altitude, land use, historical climate variety). Model performance was evaluated to identify the best predictive models, which were subsequently used to project future *O. hupensis* density under the SSP1-2.6, SSP2-4.5, and SSP5-8.5 scenarios. We further sampled 240 wild *O. hupensis* and measured their body sizes.

Results: At the individual level, we observed that larger snails had a higher survival rate at non-optimal temperatures but experienced a significant loss in body mass compared with the control group. At the population level, *O. hupensis* density closely tracks climate warming, with 91.964% of populations showing positive temperature sensitivity. Exposure during the coldest and breeding seasons had a greater influence on *O. hupensis* density with climate warming. *O. hupensis* in waterbody-dominated areas showed the largest density growth rates, whereas crop populations were the most sensitive to land cover. At the ecosystem level, only 18.968% – 24.610% of populations were expected to benefit from climate change by 2100, and these benefiting populations were concentrated in regions where sampled wild snails had a mean body size of 8.195 mm. Crop accounts for 71.953% of populations benefiting from climate warming, compared with 17.169% in forests and 8.257% in impervious-dominated areas.

Conclusion: The *O. hupensis* population benefited from climate warming but was regulated by land-use types. To mitigate the impacts of climate warming and land-use on snails, surveillance and integrated interventions should be strengthened through multi-sector collaboration.

Keywords: *Oncomelania hupensis*, Climate warming, Land use, Temperature, Time window

Introduction

Schistosomiasis is a vector-borne parasitic disease caused by blood flukes (trematode worms) of the genus S*chistosoma*. With more than 800 million people living in regions at risk of infection and over 240 million people infected, schistosomiasis ranks second after malaria in disease burden among parasitic diseases[1, 2]. In 2021, the World Health Organization (WHO) launched a strategic plan "Ending the neglect to attain the sustainable development goals: a sustainability framework for action against neglected tropical diseases 2021-2030 " with an imperative goal for member states to eliminate schistosomiasis as a public health problem by 2030[3]. However, there hasn't been as much progress as expected[4, 5]. Given that schistosomes have recently been shown to overwinter by infecting adapted intermediate host snails and to produce viable offspring when returned to optimal temperatures [6], the expansion and thriving of snail hosts have attracted considerable attention. Climate warming is considered one of the greatest threats[6-9]. Unlike tropical snails, which are likely to shrink their habitats due to narrow thermal niches, snails in temperate regions are generally considered to expand their habitats with climate warming[10].

The People's Republic of China (P.R. China) was once one of the countries most affected by schistosomiasis, with over 11 million people infected in the 1950s[11]. *S. japonicum,* infecting humans and over 40 species of wild and domestic animals[12-15], is the only *Schistosoma* species distributed in China. *Oncomelania hupensis*, as its sole intermediate snail host in China, is a prerequisite of the transmission and spread of schistosomiasis japonica[16]. Snail control has been proven to be one of the most effective tools to interrupt the lifecycle of all kind of *Schistosoma spp.* hosting human beings and WHO encourage member states to integrate snail control with conventional preventive chemotherapy programmes to reduce the prevalence and block the transmission of schistosomiasis [17, 18]. This approach has been an essential component of the Chinese national schistosomiasis control strategy since the 1950s, alongside treatment of humans and livestock, improvement of sanitation and safe water supply, disease surveillance, environmental modification, etc., and has made substantial progress in reducing both schistosomiasis prevalence and snail habitats[19, 20]. By 2023, the whole country reached the Chinese criteria of schistosomiasis transmission interruption (without new endogenous infection occurred in humans, livestock, and snails in five consecutive years)[21]. Although the area of snail habitats has been dropped sharply from 14,300 km^2 in the 1950s to 3,658 km^2 by 2024, it is noteworthy that new and re-emerging snail-infested settings have become increasing frequently, primarily driven by natural disasters such as floods or extreme drought caused by climate change in recent decades[22]. To attain China's 2030 target for schistosomiasis elimination, it is imperative to understand how climate change, especially increased temperatures, affects the distribution of *O. hupensis,* the sole intermediate host of *S. japonicum*. This understanding will thereby provide a scientific basis for formulating climate-adaptive intervention and surveillance strategies against schistosomiasis.

Previous studies have shown that *O. hupensis* is expanding its distribution to occupy suitable ecological niches along several dimensions (i.e., latitude, longitude, and altitude) in response to rising temperatures[23]. However, most studies are based mainly on mean climate, which ignores variations in climate responses across intraspecies and seasons[24, 25]. A further oversight in such studies is that climate warming involves not only a general rise in mean temperature but also shifts

in climatic extremes. These stepwise movements are also largely impacted by local habitat availability and microenvironment[26]. It is known that *O. hupensis* expansion is constrained in forests and urbans[27, 28]. *O. hupensis* densities exhibit seasonal peaks in different months, depending on the specific habitats that snails colonize[29]. Some research further suggests that climate change and land-use transitions may interact synergistically, leading to a greater effect than would be expected had they acted independently[30]. However, only a few nation-level study has examined how land use and climate warming interact to influence the population dynamics of *O. hupensis*.

Body size is also a critical trait for understanding the climatic effects on *O. hupensis*. The surface area-to-volume ratio scales with body size, affecting heat retention in ectotherms[31]. For mollusk snails, body size is closely associated with feeding behavior[32], movement[33], and even schistosome infection rate[34]. Body size could thus mediate climatic effects on *O. hupensis* directly by regulating physiological responses[32, 35], or indirectly by modulating inter- and intraspecific competitive interactions[32, 33]. Previous studies have shown variation in *O. hupensis*' body size among ecosystems[36], as well as differing body size-thermal tolerance relationships across ectothermic taxa[37], underscoring the importance of investigating this trait. Although there are some experimental studies, we provide both experimental and modeling evidence for the future change in body size of *O. hupensis*.

In this study, we combined 33 years of *O. hupensis* survey data (1990-2022) from the National Parasite Disease Prevention and Treatment Management System and schistosomiasis surveillance site reports to address the following questions spanning individual to ecosystem scales. (1) Individual level: How does body size affect the survival of *O. hupensis* under climate warming? We hypothesized that larger individuals are more likely to survive in abnormal temperatures. (2) Population level: Is there a spatial correlation between *O. hupensis* density and temperature? And which factors account for spatial variation in population-level temperature responses? We hypothesized that temperature is a key driver of *O. hupensis* density, but the magnitude and direction of this effect vary spatially. Populations that experienced greater historical temperature variability are more likely to survive ongoing climate warming; altitude imposes a geographical constraint on the expansion of *O. hupensis*; and land use adjusts local climate conditions. (3) Ecosystem level: How will *O. hupensis* respond to future climate warming and projected land-use transitions? We hypothesized that waterbodies support higher densities due to favorable habitat conditions, whereas crops support the largest populations because of their projected future expansion. From the One Health perspective, shifts in *O. hupensis* density driven by environmental change represent a critical pathway through which climate impacts human and animal health. This study will provide policymakers with insights to enable precise and effective interventions against *O. hupensis* to accelerate and consolidate the achievements of schistosomiasis control and elimination in China.

Materials and methods

O. hupensis survey data

We utilized *O. hupensis* survey data mainly collected by the National Parasite Disease Prevention and Treatment Management System. To ensure longer survey time series for as many sites as possible, we further complemented the data from literature[38-40]. These data were collected through annual field surveys conducted mainly from March to April between 1990 and 2022, using multistage sampling. The sampled population spanned latitudes from 20.58 - 35.14˚N, with the northern-most populations near the northern limit. Populations covered longitudes from 97.82 to 122.82˚E and altitudes from -8.00 m to 4,478.00 m. A total of 348,253 records were collected from 34,554 villages across 12 provinces, municipality and autonomous region: Anhui (n=2748), Fujian (n=309), Guangxi (n=427), Guangdong (n=269), Hubei (n=5738), Hunan (n=4202), Jiangsu (n=6024), and Jiangxi (n=1553), Shanghai (n=1659), Sichuan (n=4736), Yunnan (n=495), and Zhejiang (n=6394). (Additional file 1)

O. hupensis survey was conducted in combination of systematic sampling and environmental sampling methods to reduce the probability of missing infestations[41]. A systematic sampling method was employed in areas with documented *O. hupensis* occurrences over the past two years. An environmental sampling method was used in environments with no recent record of *O. hupensis* occurrences, but the snail infestation was reasonably suspected. A survey was conducted using 0.1 m^2 of sampling frames, which were systematically placed within each site. All snails within frames were collected and counted, and the survey dates were also recorded. The density of live snails was calculated using the following formula:

$$Live\ snail\ density\left(per\ m^2\right)=\frac{Total\ number\ of\ \ live\ snails}{Total\ number\ of\ \ detection\ frames\times 0.1}$$ [42]

The annual density growth rate was calculated with the following function:

$$Density\ growth\ rate_{t}=\frac{Density_{t_1}-Density_{t_2}}{Density_{t_2}\left(t_1-t_2\right)}$$

Where $Density_{t_1}$ and $Density_{t_2}$ denote population density at time t_1 and t_2, respectively.

Land-use data

We used land-use data from China's Multi-Period Land Use and Land Cover Remote Sensing Monitoring (CNLUCC) database, with a spatial resolution of 1 km^2. We included five major land-use categories: (1) Crop, (2) Forest, (3) Grass, (4) Waterbody, and (5) Impervious areas. The barren land was excluded because it includes heterogeneous conditions that are difficult to interpret. We obtained future land-use data under three scenarios generated by Zhang et al.[43]. This dataset covers the global domain at 1 km^2 grid resolution, spanning the period from 2020 to 2100.

For matching data, we created circular buffers with radii of 1km, 3km, and 5km around each site using the buffer function in the *raster* package. The proportion of each land-use type within each buffer was calculated and extracted, and the land-use type with the highest proportion was defined as the dominant land-use of its corresponding site. We presented results from the 3km buffer as the primary findings; results from the 1km and 5km buffers are presented in the Additional files.

Climate data

We used the daily minimum, mean, and maximum temperatures as the temperature variable. We downloaded the historical hourly temperature from the ERA5-Land dataset. This data provides soil temperature estimates since 1950 at a spatial resolution of 10 km^2. For each population, we extracted the hourly mean temperature for all years in which *O. hupensis* density data were available. To minimize issues with spatial autocorrelation, we also resampled the temperature data to a 1 km^2 resolution.

We then calculated the daily temperatures (minimum, mean, and maximum) for each site. We addressed missing data before the calculations. There are 1098 sites (Anhui: n=159; Guangxi: n=4; Hubei: n=120; Hunan: n=69; Jiangsu: n=55; Jiangxi: n=26; Shanghai: n=110; Sichuan: n=390; Yunnan: n=4; Zhejiang: n=161) whose locations did not overlap with the gridded dataset. We matched these sites with the temperatures in their nearest sites.

We then calculated the standardized temperature anomaly at each site as the difference between the mean annual temperature for the five years preceding the sample date and the mean annual temperature for 1901-1930 (from CRU TS version 4.09), which we used as the baseline. Here, we used the standardized temperature anomaly as a metric to estimate historical climate variability.

$$STA = \frac{T_{mean.sample} - T_{mean.baseline}}{s\left(T_{mean.baseline}\right)}$$

Where *STA* is the standardized temperature anomaly, $T_{mean.sample}$ represents the annual mean temperature over five years preceding the sample date, and $T_{mean.baseline}$ represents the annual mean temperatures for the period 1901-1930 (retrieved from CRU TS version 4.09).

Laboratory-based controlled temperature experiment

To clarify the association between body size and resilience to non-optimal temperatures, we conducted a controlled-temperature experiment using laboratory-bred adult *O. hupensis*. We first obtained 1000 *O. hupensis* from the Gongan County laboratory; these snails were maintained at -4 °C until shipment to our laboratory and then acclimated for 5 days under standard conditions (25 °C) before the experiment. Then, snails were randomly assigned to three temperature treatments: 5˚C (defined as low Temp), 25˚C (defined as control Temp), and 30˚C (defined as high Temp), with three replicates per treatment (60 snails per replicate). All tanks were maintained at suitable humidity and a 12:12 h light: dark photoperiod. All snails were continuously maintained for 45 days. To maintain suitable humidity, a sponge was placed beneath the paper on which the snails were kept. Humidity was checked every 3 hours, and water was added as needed. Body size and body weight were measured for all living individuals before and after the experiment. Snail survival was recorded every day. Between 8:00 and 9:00 am, snails were gathered to the center of the tanks and evenly sprayed with a small amount of dechlorinated water to maintain target humidity. Food was placed at the edge of each tank, and we added it every day.

Between 3:00 and 4:00 pm, motionless snails were then exposed to warm water at 40°C for 30 seconds. Individuals without reactions were regarded as dead, and their body sizes were recorded.

To examine the effect of *O. hupensis* body size on survival, we standardized initial body size using z-scores and categorized it into three classes (Small, Medium, and Large) based on the 33rd and 66th percentiles. We used the Cox proportional hazards model and Kaplan-Meier survival curves to quantify and visualize the survival patterns of *O. hupensis* across different temperature treatments and body size classes. We then grouped snails by treatment and performed log-rank tests to compare the survival differences among the three body-size classes.

Time-window modelling

O. hupensis has a well-documented one-year life cycle[36]. Given that high-temperature exposure during *O. hupensis*'s breeding period may exert a greater impact on its density than annual mean temperature exposure[29, 44], we hypothesized that the climate effects are not uniform throughout the year. To validate this hypothesis, we ran a relative sliding time-window model to provide more detailed information on seasonal variations in its climate responses. For each snail survey, we defined the survey date as the endpoint and traced back 365 days (approximating one full survival cycle of *O. hupensis*). We split this 365-day period into multiple time windows of different lengths. Within each time window, we calculated the minimum, mean, and maximum temperatures, then separately fitted a *density~temperature* model. Finally, for each population, we selected the best-supported model based on the Akaike Information Criterion (AIC).

For more model details, we applied a relative sliding time-window model to each population (snails inhabiting the same village were defined as a single population unit) to detect its temperature response using the R package *climwin*. Specifically, we first defined a time trend (year) model with an intercept as a "baseline model" using the R package *lme4*. Then, we set the parameters of our sliding window approach, including the maximum and minimum window ranges, a step of 3 days, and the aggregate statistics applied to each temperature window ("min", "mean", and "max" for minimum, mean, and maximum temperature). Finally, we ran this sliding-window analysis and used a randomization approach to account for multiple-testing-induced false positives. Scaled density was log(x+1) transformed before the analysis. Each of these model steps is described in more detail below. All models incorporated the year as a covariate to account for long-term temporal trends.

As we tested many time windows, multiple testing introduced inherent risks. To address this issue, we randomized the order of the original data within each population to remove any association between temperature and *O. hupensis* density, and then reran the sliding-window analysis. This randomization procedure was repeated 100 times, and we then compared the observed result with those from the 100 randomizations to estimate the probability of the observed result under the null hypothesis that no relationship exists between temperature and snail density. We used the $P_{\Delta AICc}$ to assess the probability that an identified time window was a false positive. $P_{\Delta AICc}$ indicates the probability of obtaining a given ΔAICc in this sliding window analysis when no relationship exists between temperature and snail density.

A relationship between temperature and *O. hupensis* density within a time window was regarded as a valid cue if $P_{\Delta AICc}$ was ≤ 0.05 (i.e., the chance of such a result occurring in a randomized

dataset was ≤5%). Time windows ≤15 days in duration were also excluded, as such short windows have been shown not to have a biological impact and can produce statistical artefacts[36]. These functions with predicted coefficients would be used to predict future *O. hupensis* densities. Here, we assessed temperature responses using three metrics: sensitivity, duration, and timing. We defined the linear coefficient calculated from a specific population as its sensitivity, the time span from window opening to window closing as duration, and the midpoint of the exposure duration as timing.

General linear mixed-effects modelling

To understand how environmental factors impact temperature responses and population dynamics (i.e., temperature sensitivity, duration, midpoint, density, and density growth rate), we ran a general linear mixed-effects model. In addition to latitude, longitude, and altitude, we included the effects of land use (i.e., crop, forest, grass, waterbody, and impervious areas), historical climate variability (standardized temperature anomaly), and their interactions as fixed effects. To account for potential spatial autocorrelation in the temperature responses and population dynamics, we used a Matérn correlation function as a random-intercept term, which estimates pairwise correlations between points as a function of their Euclidean distance, using the *spam* package in R.

To check the model's effectiveness, we generated versus-residuals plots, observed-versus-fitted plots, and Q-Q plots to evaluate whether the residuals followed a normal distribution. The models developed using mean temperature had the highest predictive accuracy, so we conducted the following analysis based on it.

Projections of the future density of *O. hupensis*

To predict future *O. hupensis* density, we obtained projected daily mean temperatures for 2025-2100 from the National Tibetan Plateau/Third Pole Environment Data Center under three IPCC climate scenarios: SSP1-2.6, SSP2-4.5, and SSP5-8.5, corresponding to low-, medium-, and high-emission pathways, respectively. Five global climate models (GCMs) of the CMIP6 ensemble were established: CMCC-ESM2, GFDL-ESM4, MPI-ESM1-2-HR, MRI-ESM2-0, and NorESM2-MM. The projected temperature data were estimated based on the ERA5 dataset.

For each GCM, we used general linear mixed-effect models to predict future temperature sensitivities, durations, and midpoints. Using these estimates and the future temperatures, we predicted *O. hupensis* density for each year from 2030 to 2100. Extreme outlier predictions were excluded to ensure reliability. For each population × year combination, we calculated the average predicted density across GCMs to enhance the robustness of predictions. We defined *O. hupensis* populations that benefit from climate warming as those whose projected densities exceeded twice the maximum historical density recorded for that population. To further validate the future change in body size, we collected 240 wild *O. hupensis* from a region predicted to harbor populations benefiting from climate warming and measured their body sizes in 2023.

All analyses were conducted in R version 4.4.2.

Result

Individual traits of *O. hupensis* under different temperature exposure

Kaplan-Meier survival analysis revealed significant differences among treatments ($p < 0.001$). In the Control group, mortality was low, with 180 snails at day 0 decreasing slightly to 163 at day 45. In contrast, the High Temp group exhibited pronounced mortality, declining from 180 to 89 snails over the same period, while the Low Temp group showed intermediate mortality, with 148 individuals surviving at day 45. (Additional file 2) Cox proportional hazards models revealed significant effects of temperature, body size, and treatment × size on survival of snails (treatment: $p < 0.001$; body-size: $p < 0.001$; treatment × size: $p < 0.05$; Additional file 3). In the High Temp and Low Temp groups, small snails were more vulnerable, whereas large individuals were more resilient. (Fig. 1a)

When comparing the body size before and 45 days after different treatments, the body size of *O. hupensis* in the High group increased from 7.100mm (95% *CI* 6.200 – 8.000) to 8.000mm (95% *CI* 7.750 – 8.250) with *p* value of 0.018, while the similar trend observed in the Low Temp group with body size increased from 7.100 mm (95% *CI* 6.200–8.000) to 8.200 mm (95% *CI* 7.780 – 8.620) with $p = 0.009$. But no significant change in body size was observed in the control group (p=0.468). (Fig. 1b; Additional file 4) In contrast, body weight decreased significantly in both the High Temp (before: 33.000 mg, 95% *CI* 27.200 – 38.800; after: 25.500 mg, 95% *CI* 21.200 – 29.800; $p = 0.025$) and Low Temp groups (before: 34.000 mg, 95% *CI* 20.500–35.500; after: 31.000 mg, 95% *CI* 24.000–38.000; $p = 0.032$), whereas snails in the control group showed a slight increase in body weight with no statistical significance (before: 28 mg, 95% *CI* 20.5–35.5; after: 31 mg, 95% *CI* 24.000–38.000; $p = 0.477$). (Fig. 1c; Additional file 4)

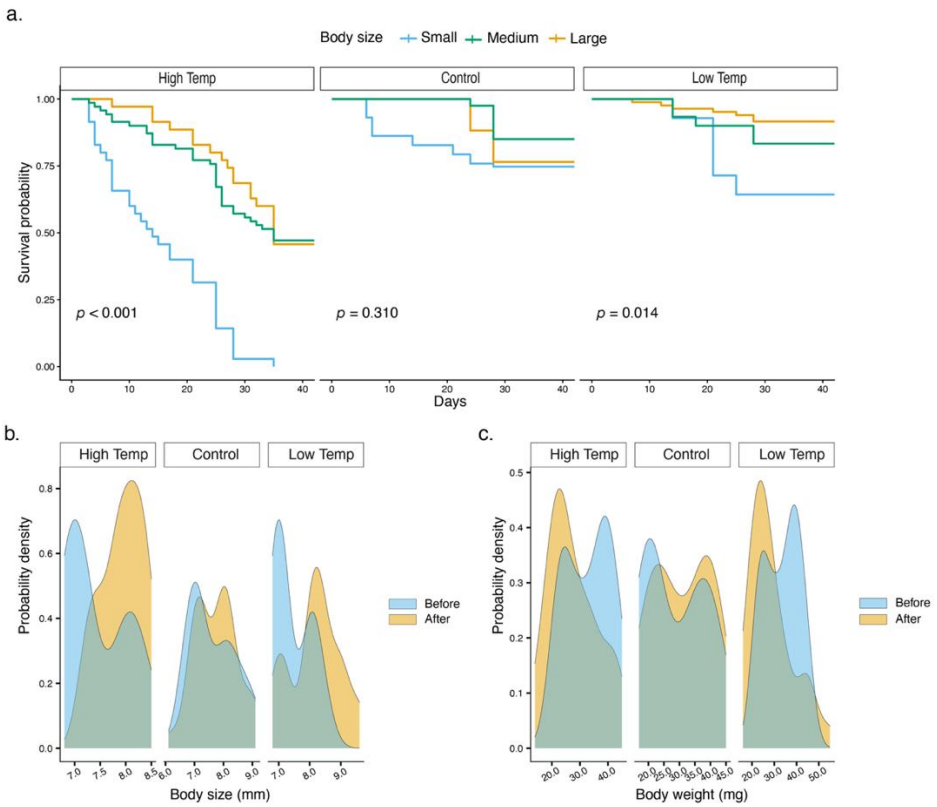


Fig 1. Effects of temperature treatments on survival, body size, and body weight of adult *O. hupensis*. a. Kaplan-Meier survival curves of adult *O. hupensis* with small, medium, and large body sizes in groups treated by

Low Temp, Control, and High Temp over the 45-day experimental period. Survival differed significantly among treatments (Log-rank test, $p < 0.001$). b. Comparison of body size before and after the experiment across the three temperature treatments. c. Comparison of body weight before and after the experiment across the three temperature treatments.

Temperature responses of the snail population

Among data collected from 34,554 villages across 12 provinces, only populations with more than 10 years of available survey data (n = 1123) were included to ensure model validity. A significant temperature response was identified in 74.176% of the filtered populations (833/1123), with the geographic distribution of these sites shown in Additional file 1. Temperature responses were detected more frequently in populations with longer records ($t = 19.732$, $p < 0.001$; Fig. 2a), suggesting that the failure to detect a temperature response after randomization is due to insufficient data rather than the absence of such a response. Of the 833 populations with a temperature response, 91.964% showed positive temperature sensitivity (Fig. 2b), with corresponding durations ranging from 23 to 220 days. (Fig. 2c)

Nearly half of the population exhibited significant temperature sensitivities during the coldest season (January–February; 46.698%), with a value of 0.027 (95% *CI* 0.003–0.051) and 0.033 (95% *CI* 0.011–0.056), respectively. Significant temperature sensitivity was also detected during the spring and autumn breeding periods (April: 27.997%; September–October: 23.152%), with effects of 0.024 (95% *CI* 0.006–0.043) and 0.035 (95% *CI* 0.002–0.068), respectively. (Fig. 2d) Seasonal variations in temperature sensitivity were additionally observed for both minimum and maximum temperatures. (Additional file 5)

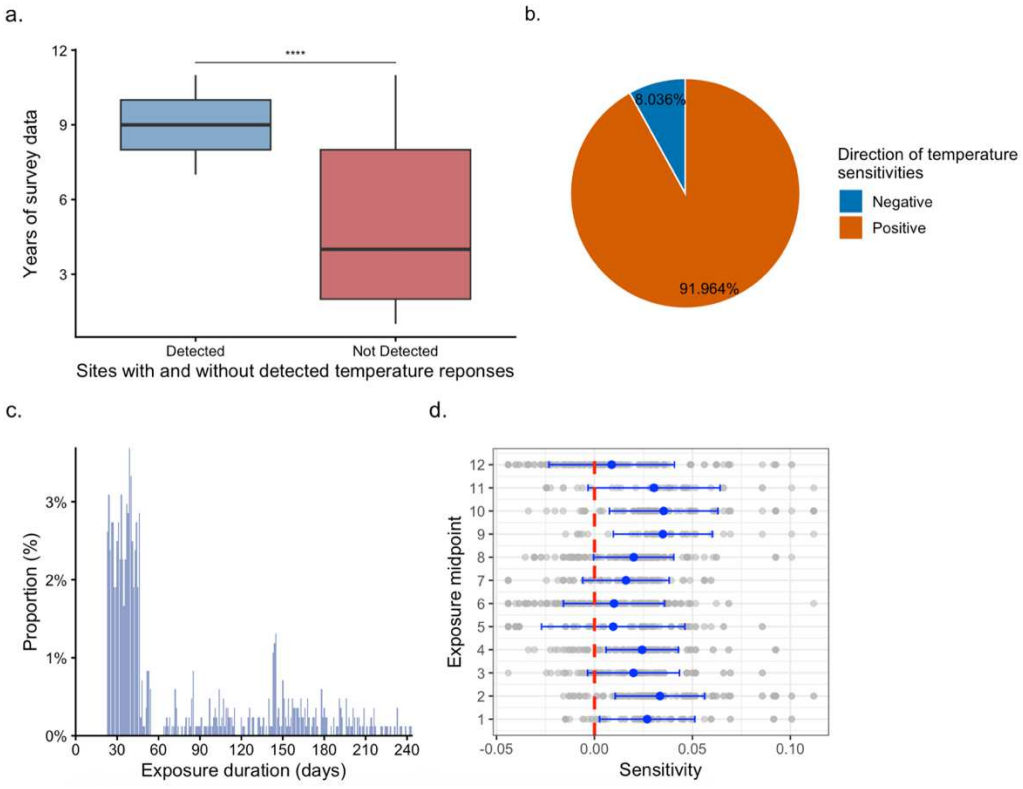


Fig 2: Characteristics of temperature responses of *O. hupensis* detected in China. a. Relationship between survey length and detection of temperature responses. b. Proportions of temperature sensitivity directions. c.

Distribution of temperature exposure duration; d. Relationship between the midpoint and sensitivity to mean temperature.

Environmental factors drive the variation of temperature responses

A distinct pattern along the latitudinal and altitudinal gradients was observed. Populations at higher latitudes and altitudes presented stronger maximum temperature sensitivity (latitude: β = 2.051×10^{-3}, *95% CI* 1.675×10^{-3}–2.415×10^{-3}; altitude: β = 1.574×10^{-5}, *95% CI* 1.412×10^{-5} – 1.732×10^{-5}; Additional file 6). Population density increased with increasing latitudes but decreased at higher altitudes (latitude: $\beta = 1.377\times10^{-2}$, *95% CI* 7.958×10^{-3} – 1.973×10^{-2}; altitude: β = -2.140×10^{-4}, *95% CI* -2.396×10^{-4} – -1.887×10^{-4}; Additional file 7). We further applied segmented linear models to identify altitudinal breakpoints in temperature sensitivity. Mean temperature sensitivity rose rapidly with increasing altitude below 13.700 m (95% *CI* 7.000 – 14.000), whereas the rate of increase slowed at higher altitudes. (Fig. 3a) In contrast, maximum temperature sensitivity increased slightly with altitude below 1663.000 m (95% *CI* 1493.900 – 1775.000), whereas it increased rapidly above this threshold. (Fig. 3b; Additional file 8)

For different land-use types, *O. hupensis* in waterbody-dominated areas had the highest density growth rate (β = 0.164, 95% *CI* 0.110 - 0.218), whereas those in other land uses had nearly the same level. (Fig. 3c; Additional file 7) In crop-dominated areas, the responses of *O. hupensis* to minimum and maximum temperatures primarily occurred in June, whereas responses to mean temperatures were concentrated later, peaking in August. *O. hupensis* inhabiting waterbodies showed their minimum and mean temperature responses mainly occurred in April, with the maximum temperatures observed in June. (Additional file 9) Notably, *O. hupensis* populations in crops were the most sensitive to land-cover change: a 1% increase in crop cover was associated with a 0.243 increase in population density. This result remained robust when analysis was conducted using 1km and 5km buffers. (Additional file 10)

Additional model results indicated that variations in temperature responses also depended on the magnitude of historical climate variability. Populations with larger standardized temperature anomalies showed weaker sensitivity to minimum and mean temperatures (minimum: β = -0.010, 95% *CI* -0.016 – -0.003; Additional file 11; mean: β = -0.021, 95% *CI* -0.027 – -0.014; Additional file 7), but stronger sensitivity to maximum temperature (maximum: β = 0.121, 95% *CI* 0.066–0.175; Additional file 6). *O. hupensis* inhabiting areas with more intensive climate variability were observed to have higher densities and growth rates (density: β = 0.280, 95% *CI* 0.194 – 0.366; growth rates: β = 0.317, 95% *CI* 0.093 – 0.537; Additional file 7). Furthermore, synergistic interactions between land-use and historical climate variability were associated with differences in temperature responses across land-use types. A warming scenario equivalent to one standard deviation of baseline temperature variation (STA = 1.0) resulted in 52.080% and 9.684% increase in *O. hupensis* densities in waterbodies and forests, respectively, compared to those in impervious areas. At the same level of climate warming, *O. hupensis* densities in grass and crops decreased by 56.440% and 15.290%, respectively. (Additional file 12) General linear mixed-effects models developed using mean temperature have a higher predictive accuracy. (Additional file 13)

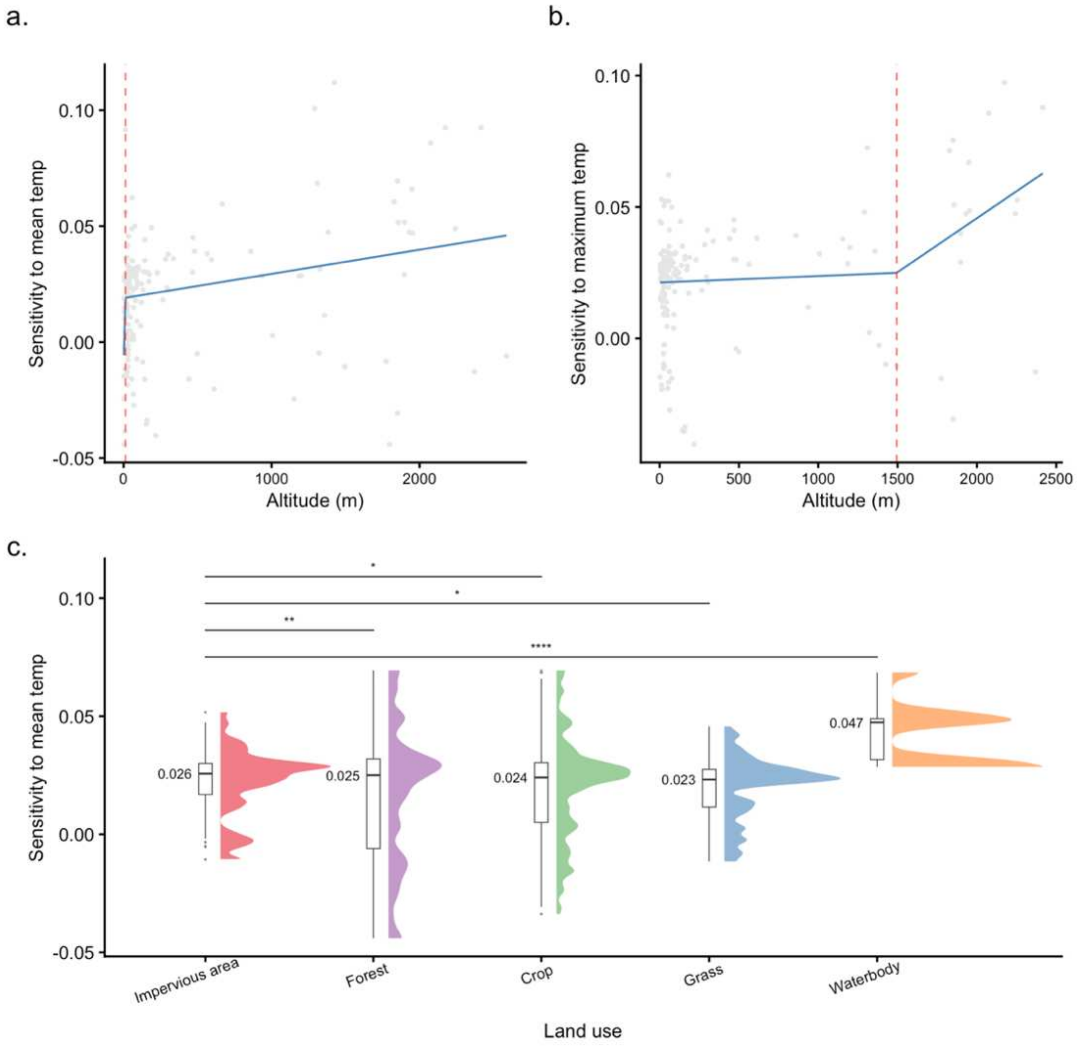


Fig 3. Geographical constraints for temperature sensitivity in *O. hupensis*. a. Segmented altitudinal patterns of sensitivity to mean temperature. b. Segmented altitudinal patterns of sensitivity to maximum temperature. c. Differences in mean temperature sensitivity among land-use types.

Prediction for future *O. hupensis* density with changes in climate and land-use

The fraction of the population benefiting from climate warming is projected to keep decreasing in the future. In 2100, these proportions will decline to 24.610% (205/833) under SSP1-2.6, 21.489% (179/833) under SSP2-4.5, and 18.968% (158/833) under SSP5-8.5, respectively. (Additional file 14) Most of these populations are projected to be distributed in the medium and lower reaches of the Yangtze River (the cross of Anhui, Jiangxi, Jiangsu, and Hubei). We further collected wild snails from five sites and measured their body sizes, which averaged 8.195 mm. (Additional file 15) Future land-use transition projections indicate that croplands would experience the largest increase in land cover, accounting for 71.953% of the population benefiting from climate warming. These differences remained robust across SSPs and GCMs. (Fig. 4a, Additional file 16) Predicted density differs significantly among land-use types (χ^2 = 73.507, p < 0.001). Under SSP1-2.6, waterbodies are projected to support the highest population densities (0.113, IQR: 0.093, 0.255), while impervious dominant areas are predicted to have the lowest densities (0.042, IQR: 0, 0.061, Fig. 4b). This ranking was consistent across all SSPs and GCMs. (Additional file 17) Across all

SSPs and GCMs, grass and impervious-dominated areas consistently showed the lowest predicted density growth rates. (Fig. 4c, Additional file 18)

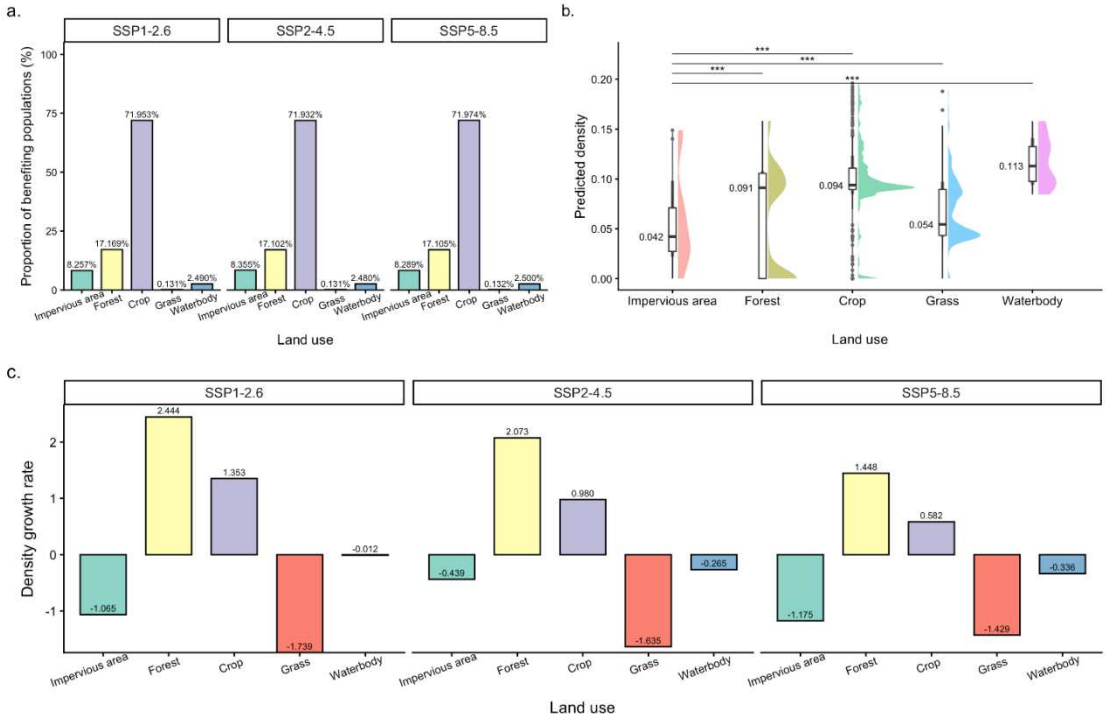


Fig 4. Land-use–specific population responses of *O. hupensis* to climatic warming under different SSPs. a. Proportion of populations benefiting from climatic warming across land-use types under SSP1–2.6, SSP2–4.5, and SSP5–8.5. b. Comparison of predicted population density among land uses under SSP1–2.6. c. Predicted density growth rate across land-uses under SSP1–2.6, SSP2–4.5, and SSP5–8.5.

Discussion

We investigated the temperature response of *O. hupensis* using long-term survey data (1990-2022). To our knowledge, this is the first study to examine the impacts of climate warming on *O. hupensis* using daily temperature variation. As expected, temperatures during the coldest season and breeding seasons significantly affected the density and growth rate of *O. hupensis*. This result underscored the importance of seasonal specialists in understanding population-level temperature sensitivities to climate warming. Consistent with previous studies, temperature sensitivity was associated with historical temperature variability, which filtered out snails with narrow thermal tolerances[45]. Geographical barriers and land use also either limit or facilitate the growth of *O. hupensis* population under global warming[46-48]. We predicted that crops would harbor the majority of *O. hupensis* populations due to ongoing agricultural expansion. Experimental results indicated that, under high temp, the mean body size of snails increased to 8.000 mm, which is very close to the mean value of snails' body size we obtained from the field snails.

A large proportion of the populations involved in the model showed positive temperature responses, indicating that temperature is a key driver of *O. hupensis* expansion. Our findings also highlight the vulnerability of numerous populations to climate warming, with negative temperature responses observed in 8.036% of the studied populations. At the individual level, we

observed disproportionate mortality among small snails, whereas larger snails had the highest survival probability under both high- and low-temperature treatments. However, this does not indicate that larger snails derive physiological benefits from extreme temperatures. Conversely, their body mass declined significantly under both high temperature and low temperature conditions, in contrast to the increase observed in the control group. The greater persistence of larger snails reflects non-physiological advantages, such as greater mobility and greater resource competitiveness. At the population level, negative latitudinal and altitudinal trends in minimum-temperature responses, and the majority of temperature responses were detected during the coldest months of the year. These results confirm that minimum temperature primarily serves as a threshold constraint rather than a direct driver of population growth[49, 50]. In addition, geographical barriers appear to constrain the expansion of *O. hupensis*: populations at higher altitudes exhibited lower densities despite showing greater temperature sensitivity.

Historical climate variability is an additional important driver of heterogeneity in temperature responses[51]. Populations experiencing greater climate variability exhibited weaker sensitivity to minimum and mean temperatures yet heightened sensitivity to maximum temperatures, suggesting that extreme temperatures may exert a more pronounced driving effect on population growth than mean temperatures[50]. Synergistic effects between land-use and climate variability further indicate that land-use provides a microclimatic buffer that modulates population temperature responses[45, 52]. At the same level of temperature rise, snail populations in waterbodies and forests exhibited increased density, whereas those in impervious-dominated areas declined. The crops were predicted to undergo the most extensive expansion among other land-use types in China[43]; consequently, they account for the largest *O. hupensis* populations nationwide. Waterbodies serve as optimal habitats for *O. hupensis*, enabling populations to experience their preferred thermal conditions during the breeding season (April to June), which is why waterbodies have the highest densities. The reason why the number of populations is not the most beneficial from climate warming may be the maximum density limitation. Forests are stable systems that respond slowly to rising temperatures but also provide a robust buffer against extreme thermal conditions.

As with any correlational study, we cannot infer causal effects; moreover, this study uses a spatial rather than a temporal analysis, and a key limitation of spatial analysis is that it cannot account for time lags in the effects of environmental change on growth rates. Furthermore, the majority of our data originated from the post 2000 period; therefore, our analysis may not comprehensively capture the historical dynamics of *O. hupensis* populations. Several analyses were conducted to enhance the robustness of our results. These included: (1) repeating the analysis across five GCMs to account for climate model uncertainty; (2) testing different SSPs to evaluate the sensitivity of predictions to socio-economic pathways; (3) performing outlier filtering to ensure that extreme values did not drive observed patterns.

Despite the limitations of correlational analyses, our results showed a clear and consistent association between *O. hupensis* temperature response and the interaction of land use and climate warming. Future work incorporating phenotypic traits and genomic analysis will provide more detailed insights into the impacts of climate change on *O. hupensis*. We did not include other aspects of climate, such as precipitation, here. In fact, temperature is considered a key climatic variable influencing the development of *O. hupensis* populations. Nevertheless, studies that

incorporate additional climatic variables and finer-scale land-use and/or land-use intensity data may yield further insights.

In conclusion, the findings in our research, consistent with previous studies[53], show that the increase in *O. hupensis* density is most pronounced in northern China, where recent climate warming represents a larger departure from historical seasonal and interannual temperature variability. Agriculturalization intensifies the impacts of *O. hupensis* expansion, whereas grass and impervious-dominated areas act as barriers. From a One Health perspective, our results underscore the interconnectedness of environmental change, snail ecology, and human health. The expansion and density increases of *O. hupensis* driven by climate warming and land-use change not only influence snail populations but also elevate the risk of schistosomiasis transmission to humans and livestock. Integrating ecological monitoring, climate modeling, and public health strategies is essential to anticipate potential outbreaks and implement timely interventions. This holistic approach highlights that effective disease control requires considering human, animal, and environmental health simultaneously. Understanding the trend of *O. hupensis* expansion and population dynamics will benefit both endemic and non-endemic areas. In all scenarios, more than 20% of the population increases its density. To eliminate schistosomiasis and consolidate the achievements obtained in China, surveillance and mitigation of the impacts of climate warming and land use on schistosomiasis, particularly intermediate snail hosts, should be strengthened to provide insights for precise intervention and resource allocation.

Additional files

Additional file 1: Plot of the distribution survey site and the sample sites of *Oncomelania hupensis.*
Additional file 2: The survival analysis of the controlled temperature experiment.
Additional file 3: Results from the Cox regression with and without temperature × body size interactions.
Additional file 4: Comparison of body sizes and body weight before and after the experiment.
Additional file 5: Relationship between the midpoint and sensitivity (results from minimum and maximum temperature).
Additional file 6: Result from general mixed function (maximum temperature).
Additional file 7: Result from general mixed function (mean temperature).
Additional file 8: Results from Segmented Linear Models.
Additional file 9: Distribution of exposure midpoint.
Additional file 10: Correlation between land use cover and *O. hupensis* density.
Additional file 11: Result from general mixed function (minimum temperature)
Additional file 12: Result from the general mixed model with interaction between land use and standardized temperature anomaly.
Additional file 13: Model diagnosis results of general linear mixed-effect models.
Additional file 14: The population benefits from global warming under SSP1-2.6, SSP2-4.5, and SSP5-8.5.
Additional file 15: Spatial distribution of populations benefiting from climate warming and wild snail sampling sites.
Additional file 16: Distribution of population benefiting from climate warming across the land-uses under SSP1-2.6, SSP2-4.5, and SSP5-8.5.

Additional file 17: Predicted density across land uses under SSP1-2.6, SSP2-4.5, SSP5-8.5.
Additional file 18: Predicted growth rate across land uses in GCMs.

Author Contributions

Qin Li and Jing Xu: The conception and design of the study, analysis, and interpretation of data, drafted the original version of the manuscript. Qin Li, Jin-Xin Zheng, Li-Juan Zhang: Acquisition of data. Qin Li, Su-ying Guo, and Ying Yang conducted the experiments. Shi-Zhu Li, Jüerg Utzinger, Xiao-Nong Zhou, and Jing Xu revised this manuscript.

Funding

This work was supported by the National Science Foundation of China (Grant No. 82073619) and the Asian Cooperation Fund Project.

Consent for publication

All authors give their consent for the publication of the present manuscript.

Competing interests

Given his role as Editor-in-Chief, Xiao-Nong Zhou had no involvement in the peer review of this article and had no access to information regarding its peer review. Full responsibility for the editorial process for this article was delegated to another journal editor. If there are other authors, they declare that they have no known competing financial interests or personal relationships that could have appeared to influence the work reported in this paper.

Declaration of generative AI use

During the preparation of this work, the author(s) used ChatGPT5 to improve readability. After using this tool/service, the author(s) reviewed and edited the content as needed and take(s) full responsibility for the content of the published article.

Data statement

Data and codes are available at https://www.scidb.cn/en/preview?dataSetId=6ad71671fa3f4fb0adc876aed01abbca&version=V1.

Reference

1. Steinmann P, Keiser J, Bos R, Tanner M, Utzinger J: Schistosomiasis and water resources development: systematic review, meta-analysis, and estimates of people at risk. Lancet Infect Dis. 2006; 6: 411-425. https://doi.org/10.1016/s1473-3099(06)70521-7.
2. GBD Results [https://vizhub.healthdata.org/gbd-results/]
3. Organization WH: Ending the neglect to attain the sustainable development goals: a sustainability framework for action against neglected tropical diseases 2021-2030. In: Ending the neglect to attain the sustainable development goals: a sustainability framework for action against neglected tropical diseases 2021-2030. edn.; 2021.
4. John R, Ezekiel M, Philbert C, Andrew A: Schistosomiasis transmission at high altitude crater lakes in western Uganda. BMC Infect Dis. 2008; 8: 110. https://doi.org/10.1186/1471-2334-8-110.

5. Boissier J, Grech-Angelini S, Webster BL, Allienne J-F, Huyse T, Mas-Coma S et al: Outbreak of urogenital schistosomiasis in Corsica (France): an epidemiological case study. The Lancet Infectious Diseases. 2016; 16: 971-979.
6. Li Y, Guo M, Jiang J, Dai R, Rebi A, Shi Z et al: Predicting Climate Change Impact on the Habitat Suitability of the Schistosoma Intermediate Host Oncomelania hupensis in the Yangtze River Economic Belt of China. Biology (Basel). 2024; 13: e1079. https://doi.org/10.3390/biology13070480.
7. van der Deure T, Maes T, Huyse T, Stensgaard AS: Climate change could fuel urinary schistosomiasis transmission in Africa and Europe. Glob Chang Biol. 2024; 30: e17434. https://doi.org/10.1111/gcb.17434.
8. Wang X, Juma S, Li W, Suleman M, Muhsin MA, He J et al: Potential risk of colonization of Bulinus globosus in the mainland of China under climate change. Infectious Diseases of Poverty. 2022; 11: 52. https://doi.org/10.1186/s40249-022-00980-2.
9. Zhou XN, Yang GJ, Yang K, Wang XH, Hong QB, Sun LP et al: Potential impact of climate change on schistosomiasis transmission in China. Am J Trop Med Hyg. 2008; 78: 188-194.
10. Newbold T, Oppenheimer P, Etard A, Williams JJ: Tropical and Mediterranean biodiversity is disproportionately sensitive to land-use and climate change. Nat Ecol Evol. 2020; 4: 1630-1638. https://doi.org/10.1038/s41559-020-01303-0.
11. Yang GJ, Zhou XN, Sun LP, Wu F, Zhong B, Qiu DC et al: Compensatory density feedback of Oncomelania hupensis populations in two different environmental settings in China. Parasit Vectors. 2011; 4: 133. https://doi.org/10.1186/1756-3305-4-133.
12. Guo Q, Chen C, Zhou K, Li Y, Tong L, Yue Y et al: Evaluation of a real-time PCR assay for diagnosis of schistosomiasis japonica in the domestic goat. Parasit Vectors. 2020; 13: 535. https://doi.org/10.1186/s13071-020-04420-8.
13. Grover E, Paull S, Kechris K, Buchwald A, James K, Liu Y et al: Predictors of bovine Schistosoma japonicum infection in rural Sichuan, China. Int J Parasitol. 2022; 52: 485-496. https://doi.org/10.1016/j.ijpara.2022.04.002.
14. Lü SB, Chen NG, Liu YM, Zhou LY, Wang YS, Hu F et al: [Survey of Schistosoma japonicum infections in wild animals in hilly transmission-controlled areas of Jiangxi Province]. Zhongguo Xue Xi Chong Bing Fang Zhi Za Zhi. 2019; 31: 463-467. https://doi.org/10.16250/j.32.1374.2019040.
15. Xu J, Li SZ, Zhang LJ, Bergquist R, Dang H, Wang Q et al: Surveillance-based evidence: elimination of schistosomiasis as a public health problem in the Peoples' Republic of China. Infect Dis Poverty. 2020; 9: 63. https://doi.org/10.1186/s40249-020-00676-5.
16. Zhou X: Report on nationwide survey of Oncomelania hupensis in China. In.: Shanghai: Shanghai Science and Techonlogy Press; 2022.
17. Lo NC, Gurarie D, Yoon N, Coulibaly JT, Bendavid E, Andrews JR et al: Impact and cost-effectiveness of snail control to achieve disease control targets for schistosomiasis. Proc Natl Acad Sci U S A. 2018; 115: E584-e591. https://doi.org/10.1073/pnas.1708729114.
18. Guidelines for laboratory and filed testing of molluscidides for control of schistosomioasis [https://www.who.int/publications/i/item/9789241515405]
19. Control OoNS: National statistics of schistosomiasis treatment and control. Shanghai, China: Office of National Schistososmiasis Control. In.; 1958.
20. Lv S, Xu J, Li YL, Bao ZP, Zhang LJ, Yang K et al: Snail control as a crucial approach to

schistosomiasis elimination: evidence from the People's Republic of China. Infect Dis Poverty. 2025; 14: 10. https://doi.org/10.1186/s40249-025-01281-0.

21. Zhang L, He J, Yang F, Dang H, Li Y, Guo S et al: [Progress of schistosomiasis control in People's Republic of China in 2023]. Zhongguo Xue Xi Chong Bing Fang Zhi Za Zhi. 2024; 36: 221-227. https://doi.org/10.16250/j.32.1374.2024116.
22. He J, Zhang L, Yang F, Dang H, Li Y, Guo S et al: [Progress of schistosomiasis control in the People's Republic of China in 2024]. Zhongguo Xue Xi Chong Bing Fang Zhi Za Zhi. 2025; 37: 223-231. https://doi.org/10.16250/j.32.1915.2025078.
23. Li YL, Dang H, Guo SY, Cao CL, Lü S, Xu J et al: [National surveillance of Oncomelania hupensis in China, 2015-2019]. Zhongguo Xue Xi Chong Bing Fang Zhi Za Zhi. 2021; 33: 127-132. https://doi.org/10.16250/j.32.1374.2020349.
24. Stensgaard AS, Vounatsou P, Sengupta ME, Utzinger J: Schistosomes, snails and climate change: Current trends and future expectations. Acta Trop. 2019; 190: 257-268. https://doi.org/10.1016/j.actatropica.2018.09.013.
25. Asare KK, Mohammed MW, Aboagye YO, Arndts K, Ritter M: Impact of Climate Change on Schistosomiasis Transmission and Distribution-Scoping Review. Int J Environ Res Public Health. 2025; 22: https://doi.org/10.3390/ijerph22050812.
26. Liu MM, Feng Y, Yang K: Impact of micro-environmental factors on survival, reproduction and distribution of Oncomelania hupensis snails. Infect Dis Poverty. 2021; 10: 47. https://doi.org/10.1186/s40249-021-00826-3.
27. Liu X, Sun Y, Yin Y, Dai X, Bergquist R, Gao F et al: Influence of urbanization on schistosomiasis infection risk in Anhui Province based on sixteen year's longitudinal surveillance data: a spatio-temporal modelling study. Infect Dis Poverty. 2023; 12: 108. https://doi.org/10.1186/s40249-023-01163-3.
28. Zhu H, Liu JB, Xiao Y, Tu ZW, Shan XW, Li B et al: Efforts to eliminate schistosomiasis in Hubei province, China: 2005-2018. Acta Trop. 2022; 231: 106417. https://doi.org/10.1016/j.actatropica.2022.106417.
29. Qi-Zhi W, Feng-Feng W, Hai Z, Cheng-Song S, Yue W, Xiao-Mei Y et al: [Dynamic change of population structure of Oncomelania hupensis]. Zhongguo Xue Xi Chong Bing Fang Zhi Za Zhi. 2017; 29: 426-430. https://doi.org/10.16250/j.32.1374.2017135.
30. Schulte To Bühne H, Tobias JA, Durant SM, Pettorelli N: Improving Predictions of Climate Change-Land Use Change Interactions. Trends Ecol Evol. 2021; 36: 29-38. https://doi.org/10.1016/j.tree.2020.08.019.
31. Harrison JF, Woods HA, Roberts SP: Ecological and Environmental Physiology of Insects: Oxford University Press; 2012.
32. Stella KA, Johnson DW: Temperature moderates the scaling relationships of energy supply and demand with body size and helps explain the Temperature-Size Rule in a marine snail. Oecologia. 2025; 207: 180. https://doi.org/10.1007/s00442-025-05816-y.
33. Hemmert HM, Baltzley MJ: Intraspecific Scaling Relationships Between Crawling Speed and Body Size in a Gastropod. Biol Bull. 2016; 230: 78-84. https://doi.org/10.1086/BBLv230n1p78.
34. Shaw KE, Cloud RE, Syed R, Civitello DJ: Parasite transmission in size-structured populations. Ecology. 2024; 105: e4221. https://doi.org/10.1002/ecy.4221.
35. Arendt J: Why get big in the cold? Size-fecundity relationships explain the temperature-size

rule in a pulmonate snail (Physa). J Evol Biol. 2015; 28: 169-178. https://doi.org/10.1111/jeb.12554.

36. Zhou X-N, Zhang, Y., Hong, Q.-B., Xu, J.-D., Wang, T.-P. (Assoc. Eds.). Yuan, Y., Wang, R.-B., Zhu, D., Zhu, H.-G., Xu, J., Sun, L.-P., Yang, K., Yang, G.-J., He, J.-C., Chen, C., Jia, T.-W., Xu, X.-J., & Liang, Y.-S.: Practical Oncomelania Snail Science; 2005.
37. Knigge T, Di Lellis MA, Monsinjon T, Köhler HR: Relevance of body size and shell colouration for thermal absorption and heat loss in white garden snails, Theba pisana (Helicidae), from Northern France. J Therm Biol. 2017; 69: 54-63. https://doi.org/10.1016/j.jtherbio.2017.06.001.
38. Gong Y, Tong Y, Jiang H, Xu N, Yin J, Wang J et al: Three Gorges Dam: the changing trend of snail density in the Yangtze River basin between 1990 and 2019. Infect Dis Poverty. 2023; 12: 45. 10.1186/s40249-023-01095-y.
39. Liu MM, Feng Y, Zhang JF, Shi L, Wang XY, Liu L et al: [Spatio-temporal patterns of Oncomelania hupensis snail habitats in Suzhou, Wuxi and Changzhou cities along the Taihu Lake region]. Zhongguo Xue Xi Chong Bing Fang Zhi Za Zhi. 2020; 32: 469-475. https://doi.org/10.16250/j.32.1374.2020222.
40. Zhou X, Dandan L, Huiming Y, Honggen C, Leping S, Guojing Y et al: Use of landsat TM satellite surveillance data to measure the impact of the 1998 flood on snail intermediate host dispersal in the lower Yangtze River Basin. Acta Trop. 2002; 82: 199-205. https://doi.org/10.1016/s0001-706x(02)00011-6.
41. Zhang LJ, Dai SM, Xue JB, Li YL, Lv S, Xu J et al: The epidemiological status of schistosomiasis in P. R. China after the World Bank Loan Project, 2002-2017. Acta Trop. 2019; 195: 135-141. https://doi.org/10.1016/j.actatropica.2019.04.030.
42. Yang K, Wang XH, Yang GJ, Wu XH, Qi YL, Li HJ et al: An integrated approach to identify distribution of Oncomelania hupensis, the intermediate host of Schistosoma japonicum, in a mountainous region in China. Int J Parasitol. 2008; 38: 1007-1016. https://doi.org/10.1016/j.ijpara.2007.12.007.
43. Zhang T, Cheng C, Wu X: Mapping the spatial heterogeneity of global land use and land cover from 2020 to 2100 at a 1 km resolution. Sci Data. 2023; 10: 748. 10.1038/s41597-023-02637-7.
44. Guo JG, Vounatsou P, Cao CL, Utzinger J, Zhu HQ, Anderegg D et al: A geographic information and remote sensing based model for prediction of Oncomelania hupensis habitats in the Poyang Lake area, China. Acta Trop. 2005; 96: 213-222. https://doi.org/10.1016/j.actatropica.2005.07.029.
45. Marshall DJ, Rezende EL, Baharuddin N, Choi F, Helmuth B: Thermal tolerance and climate warming sensitivity in tropical snails. Ecol Evol. 2015; 5: 5905-5919. https://doi.org/10.1002/ece3.1785.
46. Attwood SW, Ibaraki M, Saitoh Y, Nihei N, Janies DA: Comparative Phylogenetic Studies on Schistosoma japonicum and Its Snail Intermediate Host Oncomelania hupensis: Origins, Dispersal and Coevolution. PLoS Negl Trop Dis. 2015; 9: e0003935. https://doi.org/10.1371/journal.pntd.0003935.
47. Head JR, Chang H, Li Q, Hoover CM, Wilke T, Clewing C et al: Genetic Evidence of Contemporary Dispersal of the Intermediate Snail Host of Schistosoma japonicum: Movement of an NTD Host Is Facilitated by Land Use and Landscape Connectivity. PLoS Negl Trop Dis.

2016; 10: e0005151. https://doi.org/10.1371/journal.pntd.0005151.

48. Li Y, Guo S, Dang H, Zhang L, Xu J, Li S: Oncomelania hupensis Distribution and Schistosomiasis Transmission Risk in Different Environments under Field Conditions. Trop Med Infect Dis. 2023; 8: https://doi.org/10.3390/tropicalmed8050242.

49. Yang GJ, Vounatsou P, Zhou XN, Tanner M, Utzinger J: A potential impact of climate change and water resource development on the transmission of Schistosoma japonicum in China. Parassitologia. 2005; 47: 127-134.

50. Gaitán-Espitia JD, Belén Arias M, Lardies MA, Nespolo RF: Variation in Thermal Sensitivity and Thermal Tolerances in an Invasive Species across a Climatic Gradient: Lessons from the Land Snail Cornu aspersum. PLoS One. 2013; 8: e70662. https://doi.org/10.1371/journal.pone.0070662.

51. Pallarés S, Verberk WCEP, Bilton DT: Plasticity of thermal performance curves in a narrow range endemic water beetle. Journal of Thermal Biology. 2021; 102: 103113. https://doi.org/10.1016/j.jtherbio.2021.103113.

52. Garlaschè G, Broitman BR, Riley C, Drolet D, Howland KL, McKindsey CW et al: Local Conditions and Environmental Gradients Shape the Abundance and Size Structure of a Non-Native Intertidal Species in Atlantic North America. Ecol Evol. 2025; 15: e72532. https://doi.org/10.1002/ece3.72532.

53. Xu N, Zhang Y, Du C, Song J, Huang J, Gong Y et al: Prediction of Oncomelania hupensis distribution in association with climate change using machine learning models. Parasit Vectors. 2023; 16: 377. https://doi.org/10.1186/s13071-023-05952-5.

Supplementary Files

This is a list of supplementary files associated with this preprint. Click to download.

- Additionalfile1.docx
- Additionalfile2.docx
- Additionalfile3.docx
- Additionalfile4.docx
- Additionalfile5.docx
- Additionalfile6.docx
- FigureA1.tiff
- FigureA2.tiff
- Additionalfile7.docx
- FigureA51.tiff
- Additionalfile8.docx
- Additionalfile9.docx
- FigureA52.tiff
- Additionalfile10.docx
- FigureA15.tif
- Additionalfile11.docx
- Additionalfile12.docx
- Additionalfile13.docx
- Additionalfile14.docx
- Additionalfile15.docx
- Additionalfile16.docx
- Additionalfile17.docx
- Additionalfile18.docx